Article | Received 11 August 2026; Revised 2 October 2026; Accepted 22 October 2026; Published 26 October 2026
https://doi.org/10.55092/ae20260007

Switching-dependent prescribed performance adaptive control for switched nonlinear systems with finite-time stability

Feiyue Wu

The Key Laboratory of Intelligent Control and Optimization for Industrial Equipment, Ministry of Education, and the School of Control Science and Engineering, Dalian University of Technology, Dalian, China; E-mail: feiyue@dlut.edu.cn

Highlights:

- Mode-dependent prescribed performance bounds enable flexible tracking specifications of subsystems.
- A switching-dependent transformation addresses discontinuities induced by performance bounds at switching instants.
- Adaptive backstepping and an average dwell-time condition guarantee practical finite-time stability.
- An explicit upper bound on the settling time is derived for the switched closed-loop system.

Abstract: This paper proposes a switching-dependent prescribed performance adaptive control (SPPAC) scheme for a class of switched nonlinear systems to achieve prescribed tracking performance and practical finite-time stability. To accommodate the distinct performance requirements and dynamic characteristics of individual subsystems, switching-dependent prescribed performance bounds (PPBs) are constructed and adjusted according to the tracking error at switching instants. To address discontinuities in the transformed tracking error induced by these switching-dependent PPBs, a model transformation method is developed to reformulate the original constrained switched system as an equivalent unconstrained system. The SPPAC scheme is designed by using adaptive backstepping under an average dwell-time switching condition. Sufficient conditions are derived to guarantee the boundedness of all closed-loop signals, satisfaction of the prescribed tracking bounds, and practical finite-time convergence. Furthermore, an explicit upper bound on the settling time is established. Finally, two numerical examples are presented to demonstrate the effectiveness of the proposed SPPAC scheme.

Keywords: switched nonlinear systems; prescribed performance adaptive control; finite-time stability

1. Introduction

Switched nonlinear systems have attracted considerable attention in control theory due to their ability to capture complex dynamic behaviors arising from structural changes, variations in operating conditions, and interactions among multiple operating modes [1,2]. Such systems arise in various engineering

Copyright©2026 by the authors. Published by ELSP. This work is licensed under Creative Commons Attribution 4.0 International License, which permits unrestricted use, distribution, and reproduction in any medium provided the original work is properly cited.

applications, including power systems [3], chemical process control [4], and aerospace systems [5]. In recent years, control design with prescribed performance for switched nonlinear systems has received increasing attention [6,7]. Prescribed performance requires the tracking error to remain within predefined time-varying bounds, thereby imposing explicit specifications on convergence rate, overshoot, and steady-state accuracy [8,9]. However, the interaction between nonlinear dynamics and switching behavior makes it challenging to enforce such performance constraints across different operating modes. Furthermore, existing control approaches based on transfer-function analysis or extensive parameter tuning may be difficult to apply to switched nonlinear systems [10].

To address these challenges, prescribed performance control (PPC) has been extensively investigated for switched systems [11]. By introducing prescribed performance bounds (PPBs) and error transformation functions, the original constrained tracking problem can be reformulated as an unconstrained stabilization problem. Thus, the boundedness of the transformed error guarantees that the original tracking error remains within the PPBs [12,13]. Various PPB profiles have been developed, including exponential, hyperbolic cotangent, and finite-time performance bounds, to accommodate different control objectives [6]. Furthermore, PPC schemes have been extended to address practical issues such as modeling uncertainties [14], input saturation [15], and transition functions designed to avoid abrupt changes [16]. Despite these advances, most existing PPC methods for switched systems employ a common PPB for all subsystems. Such a uniform design imposes restrictive conditions on controller parameters and may lead to conservative or even infeasible PPC designs when subsystems exhibit different dynamic characteristics. To alleviate this limitation, PPC schemes with flexible PPBs have been proposed [17]. Although these methods can accommodate uncertain disturbances, they generally do not adjust the PPBs to meet the varying requirements of individual subsystems at switching instants. To further improve design flexibility, PPC schemes employing multi-stage PPBs have been developed [18]. However, the performance bounds in these approaches are typically predetermined and cannot be adjusted according to the tracking error at each switching instant.

On the other hand, finite-time stability (FTS) has received considerable attention, as it guarantees that the system state converges to the target equilibrium within a finite settling time [19,20]. However, for switched nonlinear systems, the presence of multiple subsystems and switching events makes the construction of a common finite-time Lyapunov function particularly challenging. Specifically, switching may disrupt the Lyapunov decrease conditions required for finite-time convergence [21], thereby complicating the direct extension of existing FTS analysis methods. Moreover, existing studies focus on establishing finite-time convergence for switched systems without considering the regulation of transient tracking performance.

In addition, system uncertainties and unknown parameters further complicate the design of finite-time PPC schemes for switched nonlinear systems [22]. For systems with unknown nonlinear dynamics, approximation-based techniques, such as fuzzy logic systems and neural networks, have been widely employed to estimate uncertain nonlinearities. Their approximation capabilities are typically supported by universal approximation results under appropriate conditions [10]. However, incorporating such approximators into control schemes that enforce prescribed transient performance and finite-time convergence may increase controller complexity and complicate stability analysis. As an alternative, adaptive laws can be employed to update parameter estimates online in the presence of unknown

parameters [23]. Nevertheless, the interplay between parameter adaptation and switching-induced discontinuities makes it more challenging to guarantee finite-time convergence and prescribed tracking performance for switched nonlinear systems.

Motivated by the above observations, this paper proposes a switching-dependent prescribed performance adaptive control (SPPAC) strategy for a class of switched nonlinear systems with practical FTS. Unlike existing approaches, the proposed SPPAC strategy employs switching-dependent PPBs that are adjusted according to the tracking error at each switching instant. This design allows mode-specific performance constraints to be imposed, thereby improving flexibility in accommodating the dynamic characteristics and performance requirements of individual subsystems. To address discontinuities in the transformed tracking error caused by switching-dependent PPBs, a model transformation technique is developed. By integrating adaptive backstepping with stability analysis based on an average dwell-time (ADT) switching, an SPPAC scheme is constructed for the considered switched nonlinear systems. Sufficient conditions are established to guarantee the boundedness of closed-loop signals, satisfaction of the prescribed transient and steady-state tracking performance, and practical finite-time convergence. Furthermore, an explicit upper bound on the settling time is derived.

The remainder of this paper is organized as follows. Section 2 formulates the control problem and presents the necessary assumptions and preliminary results. Section 3 develops the proposed SPPAC scheme, including the construction of switching-dependent PPBs, the error transformation method, and the controller design. Section 4 demonstrates the effectiveness of the proposed scheme through two numerical examples. Finally, Section 5 concludes the paper.

Notation: $\mathbb{R}^n$ denotes the n-dimensional Euclidean space. I denotes the identity matrix of appropriate dimension. For a given matrix A, A^{T} denotes its transpose, and $\|A\|$ denotes the induced matrix norm. The maximum and minimum elements of a set are denoted by $\max\{\cdot\}$ and $\min\{\cdot\}$, respectively. The Lambert W function, denoted by $\bar{W}(\cdot)$, is defined as the inverse of $f(z) = ze^z$ on a specified branch. Thus, $\bar{W}(y)e^{\bar{W}(y)} = y$ for any y in the domain of that branch.

2. Problem formulation and preliminaries

Consider a class of switched nonlinear systems described by

$$\begin{cases} \dot{\eta}_i = f_{i,\sigma}(\bar{\eta}_i, \eta_{i+1}), \quad i = 1, 2, \ldots, n-1, \\ \dot{\eta}_n = f_{n,\sigma}(\bar{\eta}_n, u), \\ y = \eta_1, \end{cases} \tag{1}$$

where $\bar{\eta}_i = [\eta_1, \ldots, \eta_i]^{\mathsf{T}} \in \mathbb{R}^i$, $i = 1, \ldots, n$, is the vector of the first i state variables, $u \in \mathbb{R}$ is the control input, and $y \in \mathbb{R}$ is the system output. The initial state is given by $\bar{\eta}_n(0) = \eta_0 \in \mathbb{R}^n$. The switching signal $\sigma : [0, \infty) \to \mathscr{M} = \{1, 2, \ldots, m\}$ is a piecewise constant, right-continuous function, where m is the number of subsystems. For each switching mode $\sigma = j \in \mathscr{M}$, $f_{i,j}(\cdot)$, $i = 1, \ldots, n$, are unknown smooth nonlinear functions that are non-affine in their last arguments.

Definition 1: For a switching signal σ, let $N_\sigma(t,T)$ denote the number of switching instants in the open interval (t,T). The switching signal σ is said to satisfy an ADT condition with $\tau_d > 0$ if there exists a chattering bound $N_0 \geq 0$ such that

$$N_\sigma(t,T) \leq N_0 + \frac{T-t}{\tau_d}, \quad \forall T > t \geq 0. \tag{2}$$

Definition 2 ([24]): Consider a system $\dot{\eta}(t) = f(\eta(t))$ with $f(0) = 0$. The system is said to achieve practical finite-time convergence if there exists a constant $\varepsilon > 0$ such that, for any initial condition $\eta(t_0)$, a finite settling time $T(\varepsilon, \eta(t_0)) < \infty$ exists satisfying

$$\|\eta(t)\| < \varepsilon, \quad \forall t \geq t_0 + T(\varepsilon, \eta(t_0)).$$

Assumption 1: The reference signal y_r is smooth, and there exists a known positive constant Y_R such that $(y_r, \dot{y}_r, \ddot{y}_r) \in \Omega_y$ for all $t \geq 0$, where

$$\Omega_y = \left\{(s_0, s_1, s_2) \in \mathbb{R}^3 : s_0^2 + s_1^2 + s_2^2 \leq Y_R\right\}.$$

Here, $\dot{y}_r$ and $\ddot{y}_r$ denote the first- and second-order time derivatives of y_r, respectively.

Assumption 2: For each $i = 1, \ldots, n$ and $j \in \mathscr{M}$, there exist unknown constants $\bar{c}_{i+1}$, $\underline{c}_{i+1}$, $\bar{h}_{i,j}$, and $\underline{h}_{i,j}$, together with unknown functions $\bar{g}_{i,j}(\cdot)$ and $\underline{g}_{i,j}(\cdot)$, such that

$$f_{i,j}(\bar{\eta}_i, \eta_{i+1}) \geq f_{i,j}(\bar{\eta}_i, 0) + \bar{g}_{i,j}(\bar{\eta}_i, \eta_{i+1})\eta_{i+1} + \bar{h}_{i,j}, \qquad \text{if } \eta_{i+1} \geq \bar{c}_{i+1}, \tag{3a}$$

$$f_{i,j}(\bar{\eta}_i, \eta_{i+1}) \leq f_{i,j}(\bar{\eta}_i, 0) + \underline{g}_{i,j}(\bar{\eta}_i, \eta_{i+1})\eta_{i+1} + \underline{h}_{i,j}, \qquad \text{if } \eta_{i+1} \leq -\underline{c}_{i+1}, \tag{3b}$$

where $\eta_{n+1} = u$. Furthermore, for $|\eta_{i+1}| \geq c_{i+1}$, where $c_{i+1} = \max\{\underline{c}_{i+1}, \bar{c}_{i+1}\}$, there exists a constant $g_{i,m} > 0$ such that

$$\min\left\{\bar{g}_{i,j}(\bar{\eta}_i, \eta_{i+1}), \underline{g}_{i,j}(\bar{\eta}_i, \eta_{i+1})\right\} \geq g_{i,m}.$$

The mean value theorem is widely employed to handle non-affine nonlinearities in control systems [25,26]. Although applicable to smooth nonlinear functions, approaches based on this theorem often impose additional restrictions on the associated partial derivatives. To avoid explicitly imposing such derivative conditions, alternative inequalities of the form (Equation (3)) have been introduced in [27,28]. These inequalities characterize the nonlinearities in two regions, namely $\eta_{i+1} \geq \bar{c}_{i+1}$ and $\eta_{i+1} \leq -\underline{c}_{i+1}$, without requiring globally uniform bounds on the corresponding partial derivatives. Similar conditions have been adopted in the control design of nonlinear systems with unknown dynamics and bounded reference signals [29,30].

Notably, Assumption 2 imposes no additional sector-type constraints on $f_{i,j}(\cdot)$ within the intermediate interval $-\underline{c}_{i+1} < \eta_{i+1} < \bar{c}_{i+1}$. Nevertheless, this flexibility introduces additional challenges in controller design. Unlike conditions that require uniformly positive control gains [24,31], Assumption 2 allows the functions $\bar{g}_{i,j}(\bar{\eta}_i, \eta_{i+1})$ and $\underline{g}_{i,j}(\bar{\eta}_i, \eta_{i+1})$ to vanish or change sign within the intermediate interval. Consequently, the corresponding gain functions are not necessarily bounded away from zero over the entire domain. Furthermore, the non-affine dependence of $f_{i,j}(\bar{\eta}_i, \eta_{i+1})$ on η_{i+1} prevents the direct application of conventional strict-feedback backstepping techniques.

The control objective is to develop a switching-dependent adaptive controller for the considered switched nonlinear systems with unknown nonlinearities such that all closed-loop signals remain bounded, the tracking error satisfies PPBs that can be adjusted according to the active switching mode, and practical finite-time convergence is achieved under an ADT switching.

Lemma 1: Let $V_{\sigma(t)}(t)$ be a positive definite function satisfying:

$$\dot{V}_j(t) \leq -\omega V_j^{1-\rho}(t) + d_1, \rho \in (0,1), \omega > 0, d_1 \geq 0 \tag{4}$$

$$V_j^{\rho}(t_k^+) \leq \mu V_{\hbar}^{\rho}(t_k^-) + d_2, \mu \geq 1, d_2 \geq 0, \tag{5}$$

where $j \in \mathscr{M}$ and the mode $\hbar$ switches to j at switching instant t_k. If the ADT switching law satisfies

$$\tau_d > \frac{\ln \mu}{\omega \rho}, \tag{6}$$

then there exists a finite time $T > 0$ such that $V_{\sigma(t)}(t) \leq (\frac{d_1}{\omega})^{\frac{1}{1-\rho}}$, $\forall t \geq T$, and an upper bound of the settling time

$$T \leq \frac{1}{\omega \rho}\left(-\bar{W}(C_1 e^{-C_2}) - C_2\right), \tag{7}$$

with the Lambert W function $\bar{W}(\cdot)$, $C_0 = \mu(\frac{d_1}{\omega})^{\frac{\rho}{1-\rho}} + d_2$, $C_1 = e^{N_0 \ln \mu}((V_{\sigma(0)} - (\frac{d_1}{\omega})^{\frac{1}{1-\rho}})^{\rho}(0) + \frac{C_0}{\mu-1})$ and $C_2 = \frac{C_0}{\mu-1}$.

Proof: Set $\bar{V} = (\frac{d_1}{\omega})^{\frac{1}{1-\rho}}$. For $V_j \geq \bar{V}$, Equation (4) yields that

$$\dot{V}_j(t) \leq -\omega V_j^{1-\rho}(t) + d_1 = -\omega V_j^{1-\rho}(t) + \omega \bar{V}^{1-\rho} = -\omega\left(V_j^{1-\rho}(t) - \bar{V}^{1-\rho}\right). \tag{8}$$

Define $W_j(t) = V_j(t) - \bar{V}$. It follows that $\dot{W}_j = \dot{V}_j \leq -\omega W_j^{1-\rho}$. Integrate Equation (8) over an active interval $[t_{k-1}, t_k]$ of the j-th mode:

$$W_j^{\rho}(t_k) \leq W_j^{\rho}(t_{k-1}) - \omega \rho (t_k - t_{k-1}). \tag{9}$$

The condition (Equation (5)) implies that

$$(W_j(t_k^+) + \bar{V})^{\rho} \leq \mu (W_{\hbar}(t_k^+) + \bar{V})^{\rho} + d_2.$$

According to the concave function property, $(a+b)^{\rho} \leq a^{\rho} + b^{\rho}$ for $a, b \geq 0$, so

$$W_j^{\rho}(t_k^+) \leq \mu W_{\hbar}^{\rho}(t_k^-) + C_0. \tag{10}$$

Let $0 = t_0 < t_1 < \cdots < t_{N_\sigma} \leq T$ be switching moments on $[0, T]$, and N_σ be the total switching number. Recursively apply Equation (9) together with Equation (10) to get

$$W_\sigma^{\rho}(T) \leq \mu^{N_\sigma}\left(W_{\sigma(0)}^{\rho}(0) + \frac{C_0}{\mu - 1}\right) - \frac{C_0}{\mu - 1} - \omega \rho \sum_{k=1}^{N_\sigma} \mu^{N_\sigma - k}(t_k - t_{k-1}).$$

With the ADT property and ADT switching law (Equation (6)), it follows that

$$W_\sigma^{\rho}(T) \leq C_1 e^{\omega \rho T} - C_2 - \omega \rho T. \tag{11}$$

With the Lambert W function [32], then $C_1e^{\omega\rho T}-C_2-\omega\rho T=0$ can be solved for $T=\frac{1}{\omega\rho}(-\bar{W}(C_1e^{-C_2})-C_2)$. It also implies that $V_\sigma^\rho(T)\leq(\frac{d_1}{\omega})^{\frac{1}{1-\rho}}$ for $T\geq\frac{1}{\omega\rho}(-\bar{W}(C_1e^{-C_2})-C_2)$. The proof is completed.

Remark 1: Lemma 1 provides a sufficient condition for the practical FTS of the switched system (Equation (1)) under ADT switching. The decay rate ω and the switching-induced growth factor μ influence the feasibility of the control design. By incorporating the nonnegative terms d_1 and d_2 into conditions (Equations (4) and (5)), respectively, the Lyapunov inequalities allow for residual effects during continuous evolution and at switching instants. This formulation provides additional flexibility in the stability analysis compared with classical FTS criteria [27,33]. Under the stated conditions, the system trajectories converge to a neighborhood of the equilibrium within finite time, with an explicit upper bound on the settling time (Equation (7)).

3. SPPAC for switched nonlinear systems

The nonaffine terms $f_{i,j}(\cdot)$ in system (Equation (1)) pose challenges for analysis and controller synthesis. The transformation introduced in [28] is used to obtain an affine-like representation in the extended state $\bar{\eta}_{i+1}$. According to Assumption 2, there exist continuous weighting functions $v_{1,i,j}(\bar{\eta}_{i+1})$, $v_{2,i,j}(\bar{\eta}_{i+1})$, $v_{3,i,j}(\bar{\eta}_{i+1})\in[0,1]$, such that

$$\begin{cases} f_{i,j}(\bar{\eta}_i,\eta_{i+1})=f_{i,j}(\bar{\eta}_i,0)+H_{i,j}(\bar{\eta}_{i+1})+G_{i,j}(\bar{\eta}_{i+1})\eta_{i+1}, \quad i=1,2,\ldots,n-1 \\ f_{n,j}(\bar{\eta}_n,u)=f_{n,j}(\bar{\eta}_n,0)+H_{n,j}(\bar{\eta}_{n+1})+G_{n,j}(\bar{\eta}_{n+1})u, \end{cases} \tag{12}$$

where $\bar{\eta}_{n+1}=[\bar{\eta}_n^\mathsf{T},u]^\mathsf{T}$. The auxiliary functions $H_{i,j}(\cdot)$ and $G_{i,j}(\cdot)$ are defined as

$$H_{i,j}(\bar{\eta}_{i+1})=\begin{cases} \bar{h}_{i,j}, \quad \text{if } \eta_{i+1}>c_{i+1}, \\ (2v_{2,i,j}(\bar{\eta}_{i+1})-1)(K_{i,j}(\bar{\eta}_i)+g_{i,m}c_{i+1}), \quad \text{if } -c_{i+1}\leq\eta_{i+1}\leq c_{i+1}, \\ \underline{h}_{i,j}, \quad \text{if } \eta_{i+1}<-c_{i+1}, \end{cases}$$

$$G_{i,j}(\bar{\eta}_{i+1})=\begin{cases} (1-v_{1,i,j}(\bar{\eta}_{i+1}))\bar{g}_{i,j}(\bar{\eta}_i,\eta_{i+1})+v_{1,i,j}(\bar{\eta}_{i+1})\bar{g}'_{i,j}(\bar{\eta}_i,\eta_{i+1}), \quad \text{if } \eta_{i+1}>c_{i+1}, \\ g_{i,m}, \quad \text{if } -c_{i+1}\leq\eta_{i+1}\leq c_{i+1}, \\ (1-v_{3,i,j}(\bar{\eta}_{i+1}))\underline{g}_{i,j}(\bar{\eta}_i,\eta_{i+1})+v_{3,i,j}(\bar{\eta}_{i+1})\underline{g}'_{i,j}(\bar{\eta}_i,\eta_{i+1}), \quad \text{if } \eta_{i+1}<-c_{i+1}. \end{cases}$$

Here, $\bar{g}'_{i,j}(\bar{\eta}_i,\eta_{i+1})=\max\{g'_{i,j},\frac{1}{c_{i+1}}(f_{i,j}(\bar{\eta}_i,\eta_{i+1})-f_{i,j}(\bar{\eta}_i,0)-\bar{h}_{i,j})\}$, $\underline{g}'_{i,j}(\bar{\eta}_i,\eta_{i+1})=\max\{g'_{i,j},\frac{-1}{c_{i+1}}\cdot(f_{i,j}(\bar{\eta}_i,\eta_{i+1})-f_{i,j}(\bar{\eta}_i,0)-\underline{h}_{i,j})\}$, $K_{i,j}(\bar{\eta}_i)\geq|f_{i,j}(\bar{\eta}_i,\eta_{i+1})-f_{i,j}(\bar{\eta}_i,0)|$ and $c_{i+1}=\max\{\underline{c}_{i+1},\bar{c}_{i+1}\}$. As a result, the switched nonlinear system (Equation (1)) can be equivalently reformulated as

$$\begin{cases} \dot{\eta}_i=f_{i,\sigma}(\bar{\eta}_i,0)+H_{i,\sigma}(\bar{\eta}_{i+1})+G_{i,\sigma}(\bar{\eta}_{i+1})\eta_{i+1}, \quad i=1,\ldots,n-1 \\ \dot{\eta}_n=f_{n,\sigma}(\bar{\eta}_n,0)+H_{n,\sigma}(\bar{\eta}_{n+1})+G_{n,\sigma}(\bar{\eta}_{n+1})u. \end{cases} \tag{13}$$

With the radial basis function (RBF) neural network technique [34], an unknown nonlinear function $F(\mathscr{Q})$ can be approximated as $F(\mathscr{Q})=W^\mathsf{T}\Phi(\mathscr{Q})$, where $W=[W_1,\ldots,W_l]^\mathsf{T}\in\mathbb{R}^l$ denotes the ideal weight vector, l is the number of basis nodes, and $\Phi(\mathscr{Q})=[\Phi_1(\mathscr{Q}),\ldots,\Phi_l(\mathscr{Q})]^\mathsf{T}\in\mathbb{R}^l$ is

the RBF vector. Each basis function $\Phi_i(\mathscr{Q})$ is selected as a Gaussian function of the form $\Phi_i(\mathscr{Q}) = \exp(-\frac{(\mathscr{Q}-\nu_i)^{\mathsf{T}}(\mathscr{Q}-\nu_i)}{\psi_i^2})$, $i = 1,\ldots,l$, where $\mathscr{Q} \in \Lambda_{\mathscr{Q}} \subset \mathbb{R}^n$ is the network input, $\Lambda_{\mathscr{Q}}$ is a compact set, $\nu_i \in \mathbb{R}^n$ denotes the center of the ith basis function, and $\psi_i > 0$ is the corresponding width. Owing to the universal approximation capability of RBF neural networks, for any given small constant $\bar{\varsigma} > 0$, there exists a weight vector $\bar{W}$ such that $F(\mathscr{Q}) = \bar{W}^{\mathsf{T}}\Phi(\mathscr{Q}) + \varsigma(\mathscr{Q})$, where the approximation error $\varsigma(\mathscr{Q})$ satisfies $|\varsigma(\mathscr{Q})| \leq \bar{\varsigma}$ for all $\mathscr{Q} \in \Lambda_{\mathscr{Q}}$.

Lemma 2 ([34]): Let $\Phi(\cdot)$ denote the basis function vector of an RBF neural network with input vector $\mathscr{Q} = [q_1,\ldots,q_n]^{\mathsf{T}}$. For the vector $\mathscr{Q}_j = [q_1,\ldots,q_j]^{\mathsf{T}}$, $1 \leq j \leq n$, the following inequality holds:

$$\|\Phi(\mathscr{Q})\| \leq \|\Phi(\mathscr{Q}_j)\|.$$

Lemma 3 ([35]): Let c_1, c_2, and c_3 be positive constants. For any $\chi, \zeta \in \mathbb{R}$, the following inequality holds:

$$|\chi|^{c_1}|\zeta|^{c_2} \leq \frac{c_1}{c_1+c_2}c_3|\chi|^{c_1+c_2} + \frac{c_2}{c_1+c_2}c_3^{-\frac{c_1}{c_2}}|\zeta|^{c_1+c_2}.$$

Lemma 4 ([36]): For $z_i \in \mathbb{R}$, $i = 1,\ldots,n$, and any $l \in (0,1)$, the following inequalities hold:

$$\left(\sum_{i=1}^{n}|z_i|\right)^l \leq \sum_{i=1}^{n}|z_i|^l \leq n^{1-l}\left(\sum_{i=1}^{n}|z_i|\right)^l.$$

We now assign a PPB to each switching mode. Let $T_1 > 0$ denote the prescribed convergence time of the performance bounds. For each subsystem $j \in \mathscr{M}$, the corresponding PPB is defined as

$$Q_j(t) = \begin{cases} (Q_{j0} - Q_F)\left(1 - \frac{t}{T_1}\right)^{\frac{1}{1-\varphi}} + Q_F, & t \in [0, T_1), \\ Q_F, & t \in [T_1, +\infty), \end{cases} \tag{14}$$

where $Q_{j0} > 0$ is the initial performance bound of subsystem j, $\varphi \in (0,1)$ is a design parameter, and $Q_F > 0$ denotes the prescribed terminal bound. In the PPC framework, Q_{j0}, Q_F, and T_1 determine the initial error bound, the terminal performance bound, and the prescribed convergence time of the performance function, respectively. Together with the positive constants $\delta_{\min}$ and $\delta_{\max}$, these parameters specify the transient and steady-state tracking requirements through the performance constraint (Equation (14)).

Remark 2: Different subsystems may have distinct transient responses and tracking performance requirements. To account for these differences, each subsystem is assigned a mode-dependent performance function $Q_j(t)$, with Q_{j0} specifying its initial performance bound. When the active mode switches from $\hbar$ to j at t_k, the prescribed bound changes from $Q_\hbar(t_k)$ to $Q_j(t_k)$. This change is determined by the switching mode rather than by an adjustment based on the instantaneous tracking error. In particular, the values of Q_{j0} are selected offline according to the dynamic characteristics and performance requirements of the individual subsystems. After T_1, all performance functions attain the common terminal value Q_F, thereby imposing the same steady-state tracking requirements on the subsystems.

Thus, the prescribed transient and steady-state tracking requirements are satisfied if the tracking error $e_y(t) = y(t) - y_r(t)$ remains within $-\delta_{\min}Q_j(t) < e_y(t) < \delta_{\max}Q_j(t)$, where $\delta_{\min}$ and $\delta_{\max}$ are positive constants. Within the PPC framework, this constrained tracking error can be mapped into an unconstrained

variable for each active subsystem. Specifically, the error transformation is defined as

$$s_j(t) = \mathscr{T}_j(e_y(t),t) = \ln \frac{\delta_{\min} + e_y(t)/Q_j(t)}{\delta_{\max} - e_y(t)/Q_j(t)}, \tag{15}$$

where $j \in \mathscr{M}$. Let $\Gamma_j(t) = e_y(t)/Q_j(t)$ denote the normalized tracking error. Differentiating Equation (15) along the trajectories of the jth subsystem gives

$$\dot{s}_j(t) = \frac{C_s}{Q_j(t)} \left(\dot{e}_y(t) - \frac{\dot{Q}_j(t)}{Q_j(t)} e_y(t) \right), \tag{16}$$

where $C_s = \frac{1}{\delta_{\min}+\Gamma_j(t)} + \frac{1}{\delta_{\max}-\Gamma_j(t)}$. According to Equations (15)–(16), the transformed error $s_j(t)$ depends on the active subsystem. As a result, $s_j(t)$ is generally discontinuous at switching instants, *i.e.*, $s_{\sigma(t_k)}(t_k) \neq s_{\sigma(t_k^-)}(t_k)$. Consider a switching instant t_k at which the active mode changes from $\hbar$ to j. The transformed errors s_j and $s_\hbar$ satisfy

$$s_j = \ln \frac{(\delta_{\min} Q_j(t_k) + \delta_{\max} Q_\hbar(t_k))e^{s_\hbar} + \delta_{\min}(Q_j(t_k) - Q_\hbar(t_k))}{(\delta_{\max} Q_j(t_k) - \delta_{\max} Q_\hbar(t_k))e^{s_\hbar} + \delta_{\max} Q_j(t_k) + \delta_{\min} Q_\hbar(t_k)},$$

which defines a continuous mapping $\bar{T}_{j,\hbar}(\cdot)$ such that $s_j = \bar{T}_{j,\hbar}(s_\hbar)$ and $\bar{T}_{j,\hbar}(0) = 0$. By the mean value theorem, for $s_\hbar \neq 0$, there exists $\varepsilon_\hbar$ lying between 0 and $s_\hbar$ such that $\bar{T}_{j,\hbar}(s_\hbar) = \bar{T}'_{j,\hbar}(\varepsilon_\hbar)s_\hbar$, where $\bar{T}'_{j,\hbar}(\cdot)$ denotes the derivative of $\bar{T}_{j,\hbar}(\cdot)$. Moreover, it follows that $\lim_{\varepsilon_\hbar \to +\infty} \bar{T}'_{j,\hbar}(\varepsilon_\hbar) = 0$, and $\lim_{\varepsilon_\hbar \to 0} \bar{T}'_{j,\hbar}(\varepsilon_\hbar) = \max_{i,j\in\mathscr{M}}\{\frac{Q_i(t_k)}{Q_j(t_k)}\}$, which implies that $\bar{T}'_{j,\hbar}(\cdot)$ is uniformly bounded. A similar boundedness result can be established for $\varepsilon_\hbar \in (-s_\hbar, 0)$ by following a similar procedure. Therefore, the switching-dependent model transformation can be expressed as

$$s_j = \bar{T}'_{j,\hbar}(\varepsilon_\hbar)s_\hbar. \tag{17}$$

Then, the PPC design proceeds by transforming the constrained tracking error into the unconstrained variable s_j through Equation (15). A coordinate transformation combined with the backstepping technique is employed to design the controller such that the transformed error s_j remains bounded, thereby guaranteeing that the tracking error remains within the PPBs. The coordinate transformation is defined as

$$\begin{aligned} z_1 &= s_1, \\ z_i &= \eta_i - \alpha_i^c, \\ \lambda_i &= \alpha_i^c - \alpha_{i-1}, \quad i = 2,3,\ldots,n, \end{aligned} \tag{18}$$

where the signal α_i^c is the output of a first-order filter introduced to avoid repeated differentiation of the virtual control law α_i. The filter dynamics are given by

$$\tau_i \dot{\alpha}_i^c + \alpha_i^c = \alpha_i, \quad \alpha_i^c(0) = \alpha_i(0), \tag{19}$$

where $\tau_i > 0$ is a constant filter time parameter. With the switching-dependent model transformation (Equation (17)), the SPPAC scheme and the adaptive laws for $j \in \mathscr{M}$ are designed as

$$u = -\frac{l_{n,j}}{g_{n,j}} z_n - \frac{z_n}{2g_{n,j}} - \frac{c_{n,j}}{2g_{n,j}} z_n \hat{\theta}_{n,j} \left\| \Phi_{n,j}(\mathscr{Q}_n) \right\|^2, \tag{20}$$

$$\dot{\hat{\theta}}_{1,j} = \frac{c_{1,j}}{2} \kappa z_1^2 \rho_j^2 \left\| \Phi_{1,j}(\mathscr{Q}_{1,j}) \right\|^2 - \hat{\theta}_{1,j}, \tag{21}$$

$$\dot{\hat{\theta}}_{i,j} = \frac{c_{i,j}}{2} \kappa z_i^2 \left\| \Phi_{i,j}(\mathscr{Q}_i) \right\|^2 - \hat{\theta}_{i,j}, \quad i = 2, \ldots, n, \tag{22}$$

where $\mathscr{Q}_{1,j} = (y_r, \dot{y}_r, Q_j, \dot{Q}_j, \eta_1)^\mathsf{T}$, $\mathscr{Q}_i = (\bar{\eta}_i, \alpha_i^c, \dot{\alpha}_i^c)^\mathsf{T}$, $\rho_j = \frac{C_s}{Q_j(t)}$ and $l_{i,j}$, $c_{i,j}$, and κ are positive design constants. The corresponding virtual control laws are given by

$$\begin{aligned} \alpha_1 &= -\frac{l_{1,j}}{\rho_j g_{1,j}} z_1 - \frac{\rho_j z_1}{2g_{1,j}} - \frac{c_{1,j}\rho_j z_1}{2g_{1,j}} \hat{\theta}_{1,j} \left\| \Phi_{1,j}(\mathscr{Q}_{1,j}) \right\|^2, \\ \alpha_i &= -\frac{l_{i,j}}{g_{i,j}} z_i - \frac{z_i}{2g_{i,j}} - \frac{c_{i,j}}{2g_{i,j}} z_i \hat{\theta}_{i,j} \left\| \Phi_{i,j}(\mathscr{Q}_i) \right\|^2, \quad i = 2, \ldots, n. \end{aligned} \tag{23}$$

Consider the Lyapunov function candidate for each subsystem of Equation (1) as

$$V_j = \sum_{i=1}^{n} \frac{1}{2} z_i^2 + \sum_{i=2}^{n} \frac{1}{2} \lambda_i^2 + \sum_{i=1}^{n} \frac{1}{2\kappa} \|\tilde{\theta}_{i,j}\|^2, \tag{24}$$

where $\kappa > 0$ is a design constant, $\hat{\theta}_{i,j}$ denotes the estimate of $\theta_{i,j}$, and $\tilde{\theta}_{i,j} = \theta_{i,j} - \hat{\theta}_{i,j}$ is the parameter estimation error. Based on the SPPAC scheme (Equations (20)–(23)), the following result holds.

Lemma 5: Along the solutions of Equations (18)–(23), for any $j, \hbar \in \mathscr{M}$, the Lyapunov function V_j satisfies

$$\dot{V}_j \leq -\omega V_j^{1-\rho} + d_1, \tag{25}$$

$$V_j \leq \mu V_\hbar + d_2, \tag{26}$$

where $\rho = \max\{\varpi_1, \varpi_2, \varpi_{3,j}\}$, $\omega = \min\{2(l_{1,j} - \frac{1}{2}), \ldots, 2(l_{n,j} - \frac{1}{2}), \frac{2}{\tau_2}, \ldots, \frac{2}{\tau_n}, 1\}$, $\mu \geq 1$, and $d_1 = \sum_{i=1}^{n} (\Xi_{i,j} + \frac{1}{2\kappa}\|\theta_{i,j}\|^2 + \frac{1}{2}M_{i-1}^{*2} + \varpi_1(1-\varpi_1)^{\frac{1-\varpi_1}{\varpi_1}} + \varpi_2(1-\varpi_2)^{\frac{1-\varpi_2}{\varpi_2}} + \varpi_{3,j}(1-\varpi_{3,j})^{\frac{1-\varpi_{3,j}}{\varpi_{3,j}}})$, $d_2 = \frac{3n}{4\kappa} \max_{i \in \{1,\ldots,n\}} \|\tilde{\theta}_{i,j} - \frac{1}{2}\tilde{\theta}_{i,\hbar}\|^2$.

Proof: The proof consists of two parts, corresponding to the switching intervals and the switching instants, respectively. Refer to Appendix A for the details.

Based on Lemmas 1 and 5, the main result of this paper is summarized as follows.

Theorem 1: Under Assumptions 1–2, consider the switched nonlinear system (Equation (1)) with the SPPAC scheme (Equation (20)), the adaptive laws (Equations (21)–(22)), and the virtual control laws (Equation (23)). If the ADT switching law (Equation (6)) is satisfied, then the following properties hold:

(S1) all signals in the closed-loop system are bounded;

(S2) the tracking error satisfies the prescribed performance constraint $-\delta_{\min} Q_j(t) < e_y(t) < \delta_{\max} Q_j(t)$, $\forall j \in \mathscr{M}, \forall t \geq 0$;

(S3) the system is FTS with an explicit settling time given in Equation (7).

Proof: Detailed derivations are provided in Appendix B.

Remark 3: The design contains two time indices, namely the convergence time T and the user-specified convergence time T_1. T characterizes the finite-time convergence of all states involved in the Lyapunov

function $V(t)$, whereas T_1 is explicitly imposed on user-specified states. Although the expression of T is analytic, it depends on several unknown parameters, which prevents the explicit computation of its exact value. In contrast, by introducing the switching-dependent PPBs, the convergence time T_1 can be directly specified by the user for selected states. This distinction separates the stability bound from the tracking-performance schedule.

Remark 4: The controller parameters can be selected according to the following guidelines. The gains $l_{i,j}$ should be chosen sufficiently large to enhance the convergence rate of the tracking error, whereas $c_{i,j}$ determine the strength of the adaptive compensation. The parameter κ adjusts the adaptation rate, and the filter constants τ_i should be selected sufficiently small to reduce the dynamic surface filtering errors. In practice, excessively large control or adaptive gains may amplify measurement noise and increase the control effort.

4. Simulation examples

Two simulation examples are presented to evaluate the performance of the proposed SPPAC scheme.

4.1. Comparison between common and switching-dependent PPB designs

The first example considers a second-order switched nonlinear system consisting of two subsystems. The nonlinear functions of the subsystems are given by $f_{1,1} = \frac{1}{2}\eta_1^4 + 0.45\eta_2 - 0.45\eta_2 e^{-1-\eta_1^2}$, $f_{2,1} = 0.1\eta_1^2 - 0.1\eta_2 + \frac{1}{2}\eta_2^2 + u$, $f_{1,2} = 0.2\eta_1^2 - 0.1\eta_1 + 0.25\eta_2$, and $f_{2,2} = 0.1\eta_1 + \cos\eta_2 + 0.1\eta_1\eta_2 + u$. The control objective is to make the system output $y = \eta_1$ track the reference signal $y_r(t) = 0.1\cos(2t)$ while satisfying the prescribed tracking performance constraints.

To examine the applicability of Assumption 2, bounding inequalities are considered for the subsystem nonlinearities with respect to η_2 and u. For the first subsystem, the proposed inequalities are $f_{1,1} \geq \eta_2(0.05\eta_1^3 + 0.05\eta_2^2) + 10$ for $\eta_2 > \frac{1}{2}$, $f_{1,1} \leq \eta_2(-5e^{\eta_1} - 5e^{\eta_2^2}) + 10$ for $\eta_2 < -\frac{1}{2}$, $f_{2,1} \geq u(-31\eta_1^2 - 18.6\eta_2^2 - 18.6u^2) + 2$ for $u > \frac{1}{2}$, and $f_{2,1} \leq u(7.434\eta_1^2 - 3.54e^{\frac{1}{2}\eta_2^2} + 11.5758u) + 2.1$ for $u < -\frac{1}{2}$. For the second subsystem, the corresponding inequalities are $f_{1,2} \geq \eta_2(-0.371\eta_1^2 - 0.119\eta_2^2) + 0.2$ for $\eta_2 > \frac{1}{2}$, $f_{1,2} \leq \eta_2(-1.4e^{1.13\eta_1^2} + 0.119\eta_2) + 0.2$ for $\eta_2 < -\frac{1}{2}$, $f_{2,2} \geq u(0.072\eta_1^2 - 0.1623\eta_2^2 + 0.0552u^2) + 0.4$ for $u > \frac{1}{2}$, and $f_{2,2} \leq u(-0.26\eta_1^2 - 0.4e^{0.1\eta_2^2} - 0.8u^2) + 0.4$ for $u < -\frac{1}{2}$. The validity of these inequalities must be established to verify Assumption 2 and justify the use of the equivalent model (Equation (13)).

The controller parameters are selected as $l = 5$, $\hbar = 2$, and $\nu = [1,2,3,4,5]^\top$ for the RBF neural network, together with $T_1 = 1.5$, $Q_{10} = 0.2$, $Q_{20} = 0.2$, $Q_F = 0.05$, $\varphi = 0.8$, $c_1 = 0.1$, $c_2 = 0.1$, $\delta_{\min} = 0.6$, $\delta_{\max} = 1.3$, $\kappa = 1$, $c_{1,1} = 0.01$, $c_{2,1} = 0.02$, $l_{1,1} = 0.01$, $l_{2,1} = 1$, $g_{1,m} = 10$, $c_{1,2} = 0.01$, $c_{2,2} = 0.05$, $l_{1,2} = 0.03$, $l_{2,2} = 0.1$, $g_{2,m} = 0.06$, and $\tau_2 = 0.05$. The initial conditions are specified as $\eta_1(0) = 0.4$, $\eta_2(0) = 0.8$, $\hat{\theta}_{1,1}(0) = 0.01$, $\hat{\theta}_{2,1}(0) = 0$, $\hat{\theta}_{1,2}(0) = 0$, and $\hat{\theta}_{2,2}(0) = 0$.

Figure 1 compares the tracking error with the common and switching-dependent PPBs. The tracking error exhibits variations in amplitude, particularly around the switching instants, reflecting the influence of the changing subsystem dynamics. In the reported simulation, the common PPB is violated near $t = 1$ s and $t = 4$ s. The interpretation of the switching-dependent PPBs, however, requires verification of the mode-specific performance parameters. Figure 2 illustrates the system output and the reference signal under the proposed SPPAC scheme. The reported maximum absolute tracking error is 0.4041. The

tracking error enters the region $|e_y(t)| \leq 0.06$ at $t = 4.48$ s and remains within this region thereafter. Over the interval $t \in [10, 15]$ s, the mean absolute tracking error and root-mean-square tracking error are 0.0090 and 0.0099, respectively. These numerical results provide quantitative measures of the tracking accuracy, while satisfaction of the prescribed performance constraints must be verified against the corresponding mode-dependent bounds.

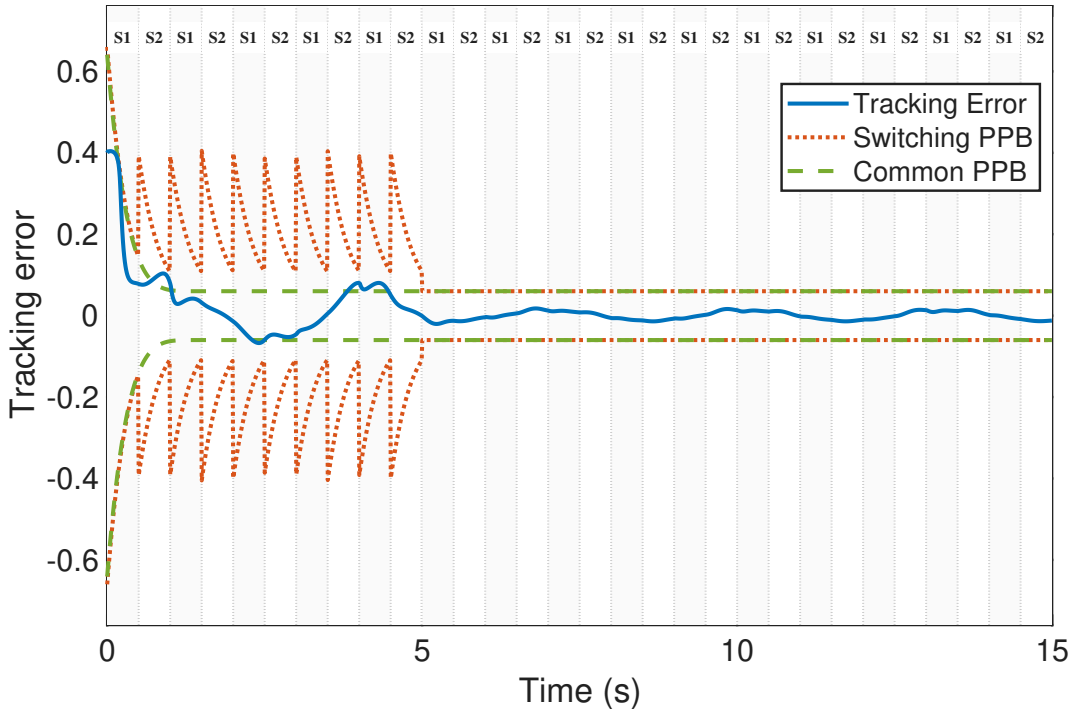

Figure 1. Tracking error with common and switching-dependent PPBs.

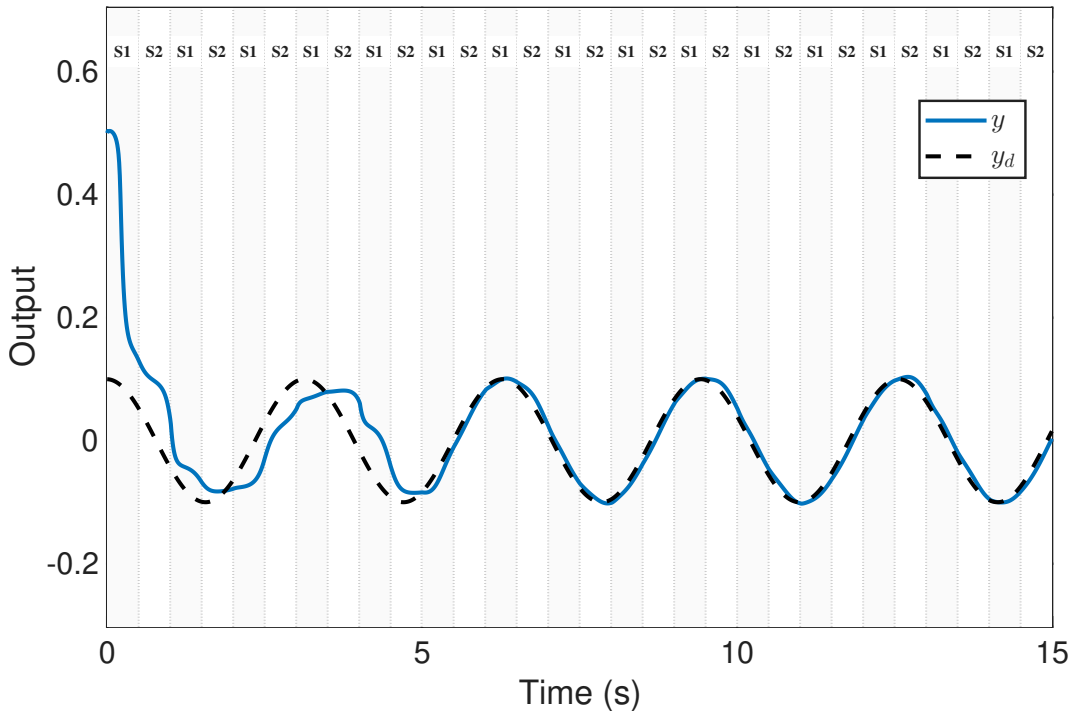

Figure 2. System output and reference signal under the proposed SPPAC scheme.

4.2. Application of the SPPAC strategy to aero-engine control

Following the system identification procedure described in [5], the aero-engine dynamics under different operating conditions are represented by switched nonlinear subsystem models. For the first operating condition, the identified model is given by

$$\begin{cases} \dot{\eta}_1 = -0.1\eta_1^4 - 1.2\eta_2 e^{-1-\eta_1^2} + 0.45\eta_2, \\ \dot{\eta}_2 = \eta_1^2 - 0.1\eta_2 - 0.3\eta_2^2 + u, \\ y = \eta_1. \end{cases}$$

The identification results yield a cost function value of 0.063, a final prediction error of 0.066, and a fitness value of 98.2%. For the second operating condition, the identified model takes the form

$$\begin{cases} \dot{\eta}_1 = -3\eta_1^2 - 3\eta_1 + 0.25\eta_2, \\ \dot{\eta}_2 = -2\eta_1 + \cos\eta_2 - 0.9\eta_1\eta_2 + u, \\ y = \eta_1. \end{cases}$$

The corresponding cost function value and final prediction error are 0.121 and 0.122, respectively, with a fitness value of 96.7%.

The controller parameters are specified as $l = 5$, $\hbar = 2$, $\nu = [1,2,3,4,5]^\top$, $T_1 = 1.5$, $Q_{10} = 0.2$, $Q_{20} = 0.2$, $Q_F = 0.08$, $\varphi = 0.75$, $c_1 = 0.1$, $c_2 = 0.1$, $\delta_{\min} = 1.6$, $\delta_{\max} = 1.6$, $\kappa = 5$, $c_{1,1} = 0.01$, $c_{2,1} = 0.02$, $l_{1,1} = 0.01$, $l_{2,1} = 0.1$, $g_{1,m} = 3.5$, $c_{1,2} = 0.01$, $c_{2,2} = 0.05$, $l_{1,2} = 0.03$, $l_{2,2} = 0.1$, $g_{2,m} = 0.05$, and $\tau_2 = 0.05$. The initial conditions are set to $\eta_1(0) = 0.4$, $\eta_2(0) = 0.8$, $\hat{\theta}_{1,1}(0) = 0.01$, $\hat{\theta}_{2,1}(0) = 0$, $\hat{\theta}_{1,2}(0) = 0$, and $\hat{\theta}_{2,2}(0) = 0$. The reference signal is chosen as $y_r(t) = 0.1\cos(2.2t)$.

Figures 3 and 4 illustrate the tracking error and output response of the aero-engine system under the proposed SPPAC scheme. The output follows the reference signal despite changes in the active subsystem, while transient tracking deviations occur during switching. The prescribed performance function reaches its terminal value Q_F at $t = T_1$, after which the performance bounds remain constant. As shown in Figure 3, the tracking error is reported to remain within the prescribed bounds throughout the simulation. The error response after $t = 5$ s further illustrates the tracking behavior under continued subsystem switching.

Figure 5 shows that the engine states converge to a bounded region within a finite time, providing numerical evidence consistent with the practical FTS (S3). As illustrated in Figure 6, the control input u exhibits noticeable fluctuations near $t = 0.5$ s and $t = 1$ s, corresponding to the transitions between subsystems. Despite these transient variations, the control input remains bounded throughout the simulation. Figure 7 presents the evolution of the mode-dependent adaptive parameter estimates, which exhibit changes associated with the switching of the active subsystem.

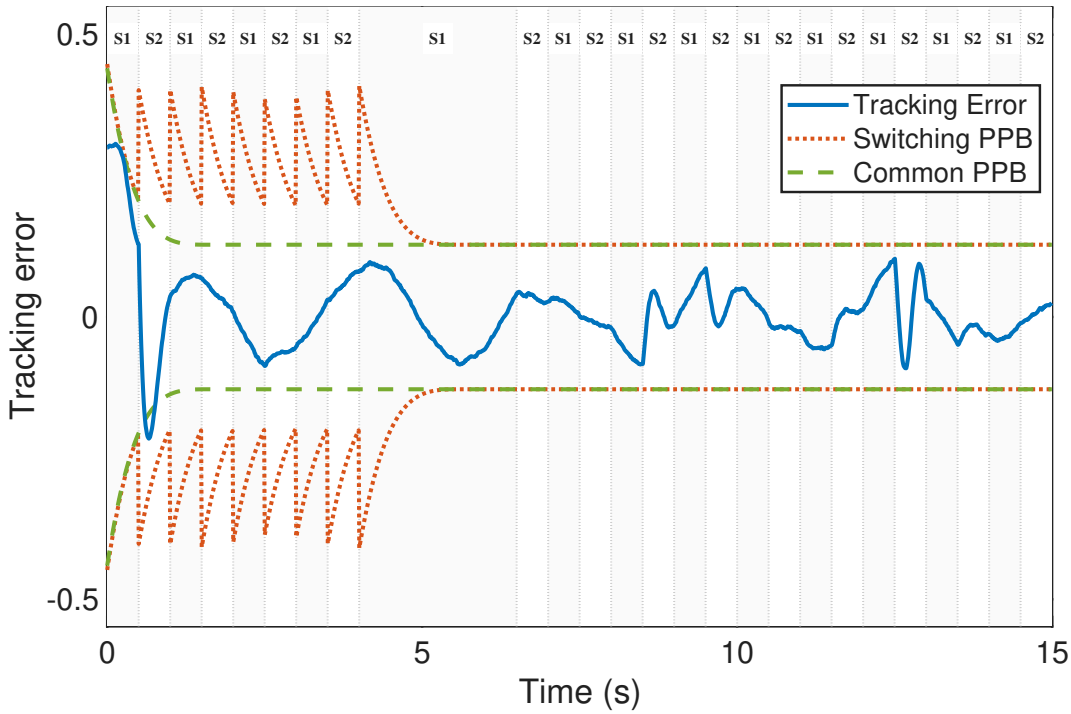

Figure 3. Tracking error and PPBs for the aero-engine system.

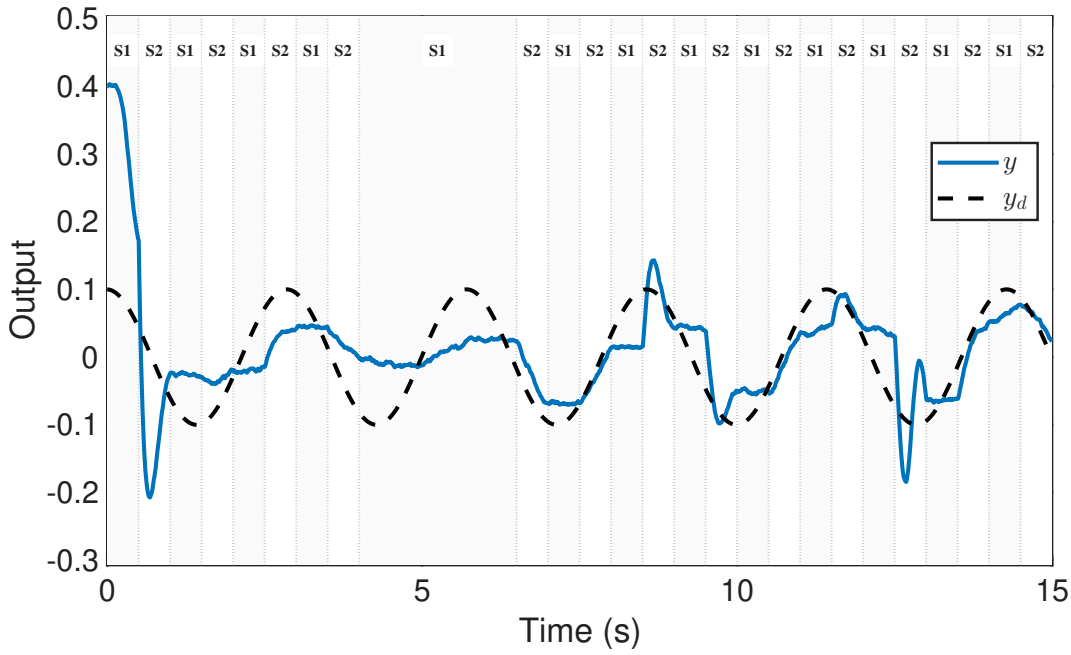

Figure 4. Aero-engine output and reference signal under the proposed SPPAC scheme.

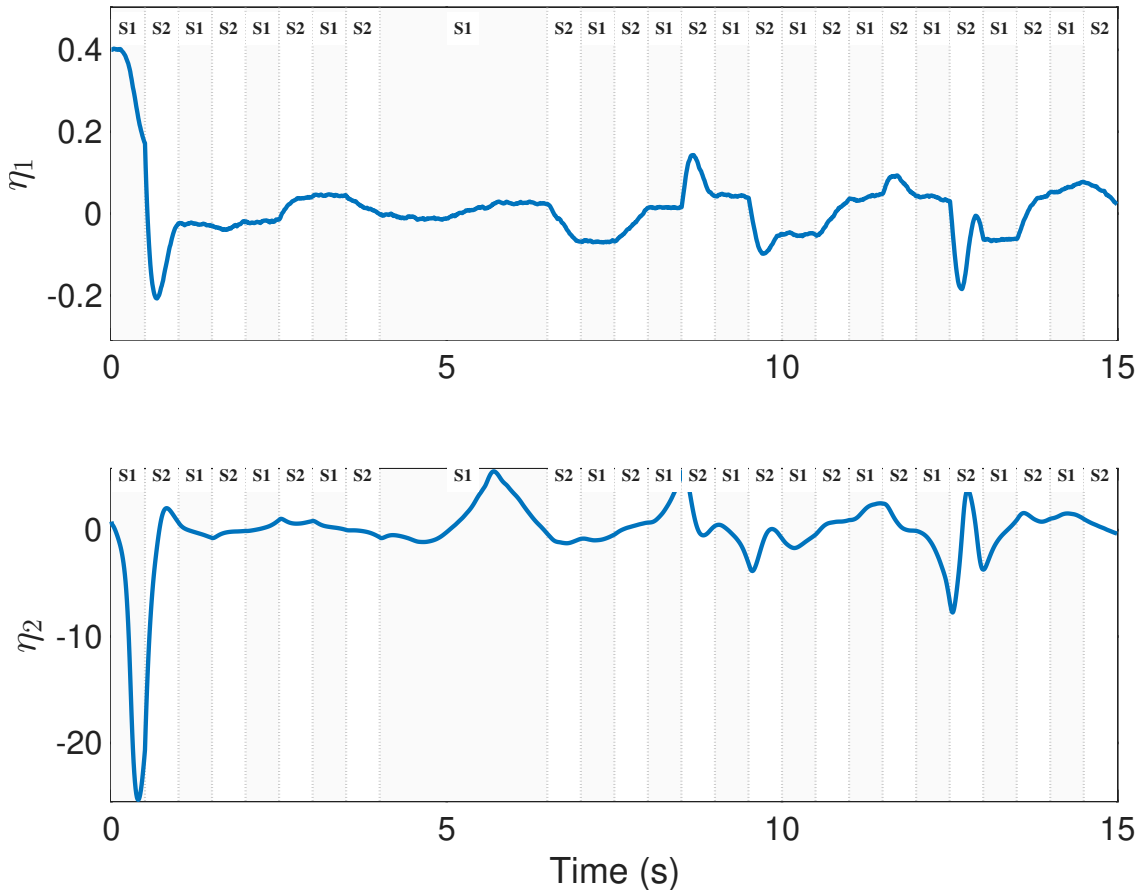

Figure 5. State responses of the aero-engine system.

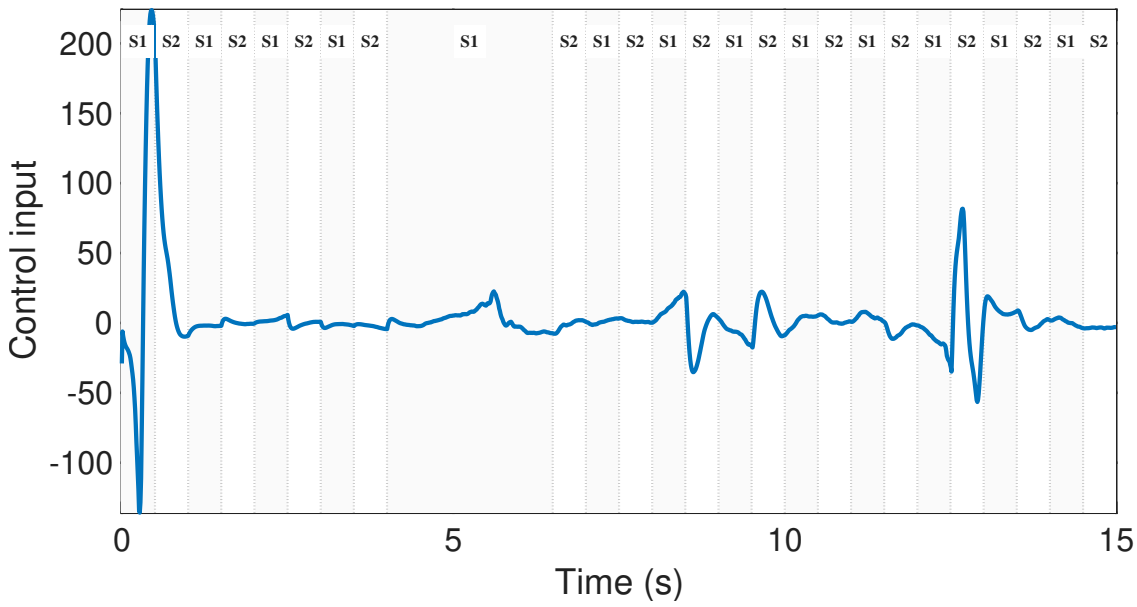

Figure 6. Control input of the aero-engine system.

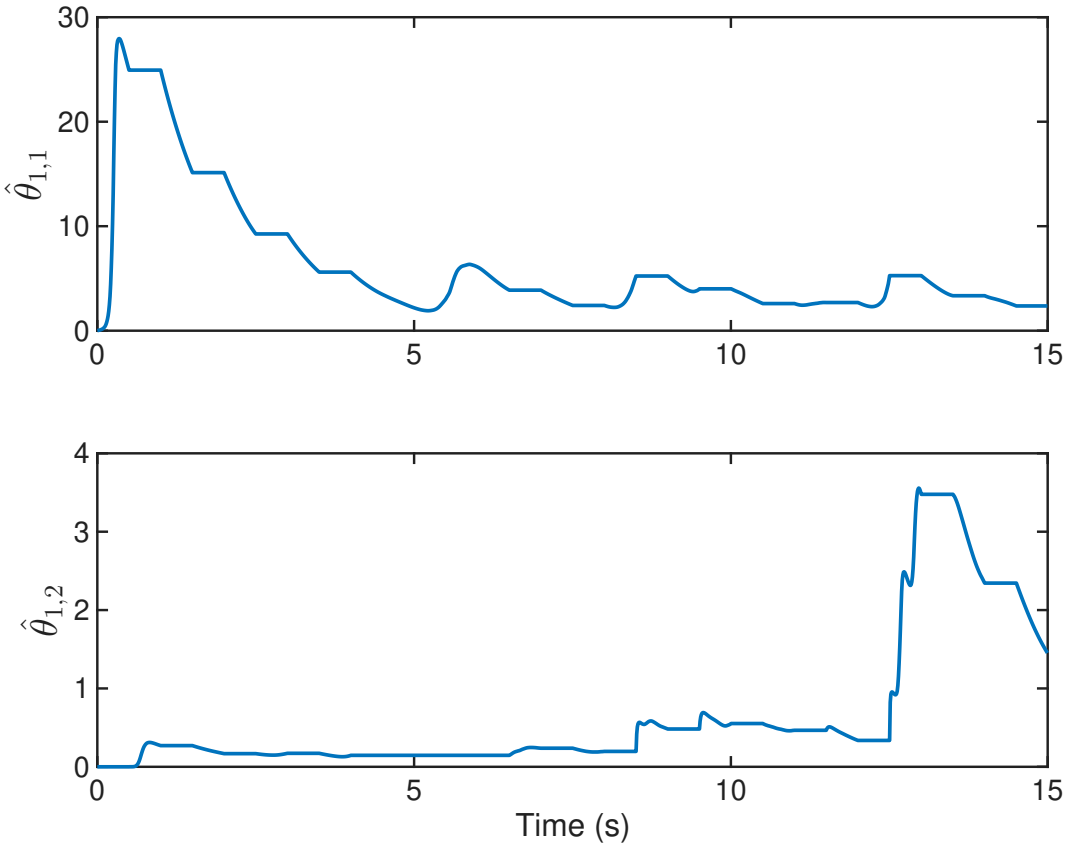

Figure 7. Adaptive parameter estimates of the aero-engine system.

5. Conclusion

This paper has developed an SPPAC scheme for a class of switched nonlinear systems to achieve prescribed tracking performance and practical FTS. By introducing switching-dependent PPBs, the proposed scheme allows different subsystems to satisfy their respective transient performance requirements. To address the discontinuities in the transformed tracking error, a switching-dependent model transformation has been established to transform the constrained tracking problem into an unconstrained formulation. An adaptive backstepping controller has then been designed, with the stability analysis conducted under an ADT condition. Sufficient conditions have been formulated to ensure the boundedness of closed-loop signals, satisfaction of the prescribed tracking constraints, and practical finite-time convergence. An explicit upper bound on the settling time has also been derived.

Data availability statement

No datasets were generated or analysed during the current study.

Declaration of generative AI and AI-assisted technologies

During the preparation of this manuscript, ChatGPT (OpenAI) was only used for language polishing, grammar checking and readability improvement. The author has fully reviewed and revised all AI-generated texts, and takes full responsibility for the content of the manuscript, including all interpretations and conclusions. No AI tool was involved in study design, data collection, data analysis or drawing scientific conclusions.

Acknowledgments

The author would like to thank the editors and anonymous reviewers for their valuable comments and suggestions, which greatly improved the quality of this manuscript.

Conflicts of interest

The author declares that there is no known competing financial interests or personal relationships that could have appeared to influence the work reported in this paper.

Appendix A. Proofs of Lemma 5

Define the Lyapunov function candidate $V_{1,j} = \frac{1}{2}z_1^2 + \frac{1}{2\kappa}\tilde{\theta}_{1,j}^{\mathsf{T}}\tilde{\theta}_{1,j}$. Invoking Equations (13), (16), and (18), the time derivative of $V_{1,j}$ along the system trajectories is given by

$$\dot{V}_{1,j} = z_1\rho_j\left(f_{1,j}(\bar{\eta}_1,0) + H_{1,j}(\bar{\eta}_2) + G_{1,j}(\bar{\eta}_2)\left(z_2+\lambda_2+\alpha_1\right) - \dot{y}_r - \frac{\dot{Q}_j(t)}{Q_j(t)}e_y\right) - \frac{1}{\kappa}\tilde{\theta}_{1,j}^{\mathsf{T}}\dot{\hat{\theta}}_{1,j}. \tag{27}$$

From Equation (12), it follows that $H_{1,j}(\bar{\eta}_2) \le K_{1,j}(\bar{\eta}_2) + h_{1,j}$, where $h_{1,j} = \max\{g_{1,m}c_2, \underline{h}_{1,j}, \bar{h}_{1,j}\}$. Then, for any given constant $\delta_{1,j} > 0$, one has

$$z_1\rho_j H_{1,j}(\bar{\eta}_2) \le \frac{\delta_{1,j}}{2}z_1^2\rho_j^2\left(K_{1,j}^2(\bar{\eta}_2) + h_{1,j}^2\right) + \frac{1}{2\delta_{1,j}}. \tag{28}$$

Moreover, by Young's inequality, it holds that

$$z_1\rho_j G_{1,j}(\bar{\eta}_2)(z_2+\lambda_2+\alpha_1) \le z_1\rho_j G_{1,j}(\bar{\eta}_2)\alpha_1 + z_1^2\rho_j^2 G_{1,j}^2(\bar{\eta}_2) + \frac{1}{2}z_2^2 + \frac{1}{2}\lambda_2^2. \tag{29}$$

Substituting Equations (28) and (29) into Equation (27) yields

$$\dot{V}_{1,j} \le z_1\rho_j\left(F_{1,j}(\bar{\mathscr{Q}}_{1,j}) + G_{1,j}(\bar{\eta}_2)\alpha_1\right) + \frac{1}{2\delta_{1,j}} + \frac{1}{2}z_2^2 + \frac{1}{2}\lambda_2^2 - \frac{1}{\kappa}\tilde{\theta}_{1,j}^{\mathsf{T}}\dot{\hat{\theta}}_{1,j} \tag{30}$$

where $F_{1,j}(\bar{\mathscr{Q}}_{1,j}) = f_{1,j}(\eta_1,0) + \frac{\delta_{1,j}}{2}z_1\rho_j(K_{1,j}^2(\bar{\eta}_2) + h_{1,j}^2) + z_1\rho_j G_{1,j}^2(\bar{\eta}_2) - \dot{y}_r - \frac{\dot{Q}_j(t)}{Q_j(t)}e_y$ and $\bar{\mathscr{Q}}_{1,j} = (y_r, \dot{y}_r, Q_j, \dot{Q}_j, \eta_1, \eta_2)^{\mathsf{T}}$. The unknown nonlinear function $F_{1,j}(\bar{\mathscr{Q}}_{1,j})$ is approximated by an RBF neural network, and the approximation error $\varepsilon_{1,j}(\mathscr{Q}_{1,j})$ satisfies $|\varepsilon_{1,j}(\mathscr{Q}_{1,j})| \le \varepsilon_1$. According to Lemma 2, one has

$$z_1\rho_j F_{1,j}(\bar{\mathscr{Q}}_{1,j}) \le \frac{c_{1,j}}{2}z_1^2\rho_j^2\theta_{1,j}\left\|\Phi_{1,j}(\mathscr{Q}_{1,j})\right\|^2 + \frac{1}{2c_{1,j}} + \frac{1}{2}z_1^2\rho_j^2 + \frac{\varepsilon_1^2}{2} \tag{31}$$

where $\theta_{1,j} = \|\vartheta_{1,j}\|^2$. Substituting Equation (31) into Equation (30) yields

$$\begin{aligned}\dot{V}_{1,j} \le & z_1\rho_j\left(G_{1,j}(\bar{\eta}_2)\alpha_1 + \frac{1}{2}z_1\rho_j + \frac{c_{1,j}}{2}z_1\rho_j\hat{\theta}_{1,j}\left\|\Phi_{1,j}(\mathscr{Q}_{1,j})\right\|^2\right) \\ & + \frac{1}{2}z_2^2 + \frac{1}{2}\lambda_2^2 - \frac{1}{\kappa}\tilde{\theta}_{1,j}^{\mathsf{T}}\dot{\hat{\theta}}_{1,j} + \Xi_{1,j}.\end{aligned} \tag{32}$$

where $\Xi_{1,j} = \frac{1}{2c_{1,j}} + \frac{\varepsilon_1^2}{2} + \frac{1}{2\delta_{1,j}}$. With the adaptive law (Equation (21)) and the virtual control law (Equation (23)), it follows from Equation (32) that

$$\dot{V}_{1,j} \leq -l_{1,j}z_1^2 + \frac{1}{2}z_2^2 + \frac{1}{2}\lambda_2^2 + \frac{1}{\kappa}\tilde{\theta}_{1,j}^{\top}\hat{\theta}_{1,j} + \Xi_{1,j}. \tag{33}$$

Define the Lyapunov function candidate recursively as $V_{i,j} = V_{i-1,j} + \frac{1}{2}z_i^2 + \frac{1}{2}\lambda_i^2 + \frac{1}{2\kappa}\tilde{\theta}_{i,j}^{\top}\tilde{\theta}_{i,j}$, for $i = 2,\ldots,n-1$. By combining Equations (13), (18), and (19), the time derivative of $V_{i,j}$ along the system trajectories is given by

$$\begin{aligned}\dot{V}_{i,j} =& \dot{V}_{i-1,j} + z_i\left(f_{i,j}(\bar{\eta}_i,0) + H_{i,j}(\bar{\eta}_{i+1}) + G_{i,j}(\bar{\eta}_{i+1})\left(z_{i+1}+\lambda_{i+1}+\alpha_i\right) - \dot{\alpha}_i^c\right)\\ &+ \lambda_i\left(-\frac{\lambda_i}{\tau_i} - \dot{\alpha}_{i-1}\right) - \frac{1}{\kappa}\tilde{\theta}_{i,j}^{\top}\dot{\hat{\theta}}_{i,j}.\end{aligned} \tag{34}$$

Applying Young's inequality yields

$$\begin{aligned}& z_iG_{i,j}(\bar{\eta}_{i+1})\left(z_{i+1}+\lambda_{i+1}+\alpha_i\right)\\ \leq& z_iG_{i,j}(\bar{\eta}_{i+1})\alpha_i + z_i^2G_{i,j}^2(\bar{\eta}_{i+1}) + \frac{1}{2}z_{i+1}^2 + \frac{1}{2}\lambda_{i+1}^2 z_iH_{i,j}(\bar{\eta}_{i+1})\\ \leq& \frac{\delta_{i,j}}{2}z_i^2\left(K_{i,j}^2(\bar{\eta}_{i+1}) + h_{i,j}^2\right) + \frac{1}{2\delta_{i,j}}\end{aligned}$$

where $h_{i,j} = \max\{g_{i,m}c_{i+1}, \underline{h}_{i,j}, \bar{h}_{i,j}\}$ and $\delta_{i,j} > 0$ is a design constant. Substituting the above inequalities into Equation (34) yields

$$\begin{aligned}\dot{V}_{i,j} \leq& \dot{V}_{i-1,j} + z_i\left(F_{i,j}(\bar{\mathscr{Q}}_i) + G_{i,j}(\bar{\eta}_{i+1})\alpha_i\right) + \lambda_i\left(-\frac{\lambda_i}{\tau_i} + M_{i-1}(\cdot)\right)\\ &+ \frac{1}{2\delta_{i,j}} + \frac{1}{2}z_{i+1}^2 + \frac{1}{2}\lambda_{i+1}^2 - \frac{1}{\kappa}\tilde{\theta}_{i,j}^{\top}\dot{\hat{\theta}}_{i,j}\end{aligned} \tag{35}$$

where $M_{i-1}(\cdot) = -\dot{\alpha}_{i-1}$, $F_{i,j}(\bar{\mathscr{Q}}_i) = f_{i,j}(\bar{\eta}_i,0) + \frac{\delta_{i,j}}{2}z_i(K_{i,j}^2(\bar{\eta}_i) + h_{i,j}^2) + z_iG_{i,j}^2(\bar{\eta}_{i+1}) - \dot{\alpha}_i^c$ and the RBF approximation error satisfies $|\varepsilon_{i,j}(\mathscr{Q}_i)| \leq \varepsilon_i$. According to Lemma 2, it follows that

$$z_iF_{i,j}(\bar{\mathscr{Q}}_i) \leq \frac{c_{i,j}}{2}z_i^2\theta_{i,j}\left\|\Phi_{i,j}(\mathscr{Q}_i)\right\|^2 + \frac{1}{2c_{i,j}} + \frac{1}{2}z_i^2 + \frac{\varepsilon_i^2}{2} \tag{36}$$

where $\theta_{i,j} = \|\vartheta_{i,j}\|^2$. Substituting Equation (36) into Equation (35) yields

$$\begin{aligned}\dot{V}_{i,j} \leq& \dot{V}_{i-1,j} + \lambda_i\left(-\frac{\lambda_i}{\tau_i} + M_{i-1}(\cdot)\right) + z_i\left(\frac{1}{2}z_i + \frac{c_{i,j}}{2}z_i\theta_{i,j}\left\|\Phi_{i,j}(\mathscr{Q}_i)\right\|^2 + G_{i,j}(\bar{\eta}_{i+1})\alpha_i\right)\\ &+ \frac{1}{2}z_{i+1}^2 + \frac{1}{2}\lambda_{i+1}^2 - \frac{1}{\kappa}\tilde{\theta}_{i,j}^{\top}\dot{\hat{\theta}}_{i,j} + \Xi_{i,j}\end{aligned} \tag{37}$$

where $\Xi_{i,j} = \frac{1}{2c_{i,j}} + \frac{\varepsilon_i^2}{2} + \frac{1}{2\delta_{i,j}}$. With the adaptive law (Equation (22)) and the virtual control law (Equation (23)), it follows from Equation (37) that

$$\dot{V}_{i,j} \leq \dot{V}_{i-1,j} - l_{i,j}z_i^2 + \lambda_i\left(-\frac{\lambda_i}{\tau_i} + M_{i-1}(\cdot)\right) + \frac{1}{2}z_{i+1}^2 + \frac{1}{2}\lambda_{i+1}^2 + \frac{1}{\kappa}\tilde{\theta}_{i,j}^{\top}\hat{\theta}_{i,j} + \Xi_{i,j}. \tag{38}$$

The Lyapunov function candidate for the j-th subsystem is chosen as $V_j = V_{n-1,j} + \frac{1}{2}z_n^2 + \frac{1}{2}\lambda_n^2 + \frac{1}{2\kappa}\tilde{\theta}_{n,j}^{\top}\tilde{\theta}_{n,j}$. Taking the time derivative of V_j along the system trajectories and invoking Equations (13), (18), (19) yields

$$\dot{V}_j = \dot{V}_{n-1,j} + \lambda_n \left(-\frac{\lambda_n}{\tau_n} + M_{n-1}(\cdot) \right) - \frac{1}{\kappa} \tilde{\theta}_{n,j}^{\mathsf{T}} \dot{\hat{\theta}}_{n,j}$$
$$+ z_n \left(f_{n,j}(\bar{\eta}_n, 0) + H_{n,j}(\bar{\eta}_{n+1}) + G_{n,j}(\bar{\eta}_{n+1}) u - \dot{\alpha}_n^c \right) \tag{39}$$

where $M_{n-1}(\cdot) = -\dot{\alpha}_{n-1}$. Define $F_{n,j}(\bar{\mathscr{Q}}_n) = f_{n,j}(\bar{\eta}_n, 0) + \frac{\delta_{n,j}}{2} z_n (K_{n,j}^2(\bar{\eta}_n) + h_{n,j}^2) - \dot{\alpha}_n^c$ and assume that the approximation error satisfies $|\varepsilon_{n,j}(\bar{\mathscr{Q}}_n)| \leq \varepsilon_n$. According to Lemma 2, one has

$$z_n F_{n,j}(\bar{\mathscr{Q}}_n) \leq \frac{c_{n,j}}{2} z_n^2 \theta_{n,j} \left\| \Phi_{n,j}(\mathscr{Q}_n) \right\|^2 + \frac{1}{2c_{n,j}} + \frac{1}{2} z_n^2 + \frac{\varepsilon_n^2}{2} \tag{40}$$

where $\theta_{n,j} = \|\vartheta_{n,j}\|^2$. Substituting Equation (40) into Equation (39) yields

$$\dot{V}_j \leq \dot{V}_{n-1,j} + \lambda_n \left(-\frac{\lambda_n}{\tau_n} + M_{n-1}(\cdot) \right) - \frac{1}{\kappa} \tilde{\theta}_{n,j}^{\mathsf{T}} \dot{\hat{\theta}}_{n,j} + \Xi_{n,j}$$
$$+ z_n \left(\frac{c_{n,j}}{2} z_n \theta_{n,j} \left\| \Phi_{n,j}(\mathscr{Q}_n) \right\|^2 + \frac{1}{2} z_n + G_{n,j}(\bar{\eta}_{n+1}) u \right) \tag{41}$$

where $\Xi_{n,j} = \frac{1}{2c_{n,j}} + \frac{\varepsilon_n^2}{2} + \frac{1}{2\delta_{n,j}}$. With the adaptive law (Equation (22)) and the actual control input Equation (20), it follows from Equation (41) that

$$\dot{V}_j \leq \dot{V}_{n-1,j} - l_{n,j} z_n^2 + \lambda_n \left(-\frac{\lambda_n}{\tau_n} + M_{n-1}(\cdot) \right) + \frac{1}{\kappa} \tilde{\theta}_{n,j}^{\mathsf{T}} \hat{\theta}_{n,j} + \Xi_{n,j}. \tag{42}$$

According to [37], there exist positive constants M_{i-1}^*, $i = 2, \ldots, n$, such that $M_{i-1}(\cdot) \leq M_{i-1}^*$. Applying Young's inequality yields $\lambda_i M_{i-1}(\cdot) \leq \frac{1}{2}\lambda_i^2 + \frac{1}{2} M_{i-1}^{*2}$, $\frac{1}{\kappa} \tilde{\theta}_{i,j}^{\mathsf{T}} \hat{\theta}_{i,j} \leq \frac{1}{2\kappa} \hat{\theta}_{i,j}^{\mathsf{T}} \hat{\theta}_{i,j} - \frac{1}{2\kappa} \tilde{\theta}_{i,j}^{\mathsf{T}} \tilde{\theta}_{i,j}$. By Lemma 3, one has

$$\sum_{i=1}^{n} \left(\frac{1}{2} z_i^2 \right)^{1-\varpi_1} \leq \sum_{i=1}^{n} \frac{1}{2} z_i^2 + \varpi_1 (1 - \varpi_1)^{\frac{1-\varpi_1}{\varpi_1}}, \tag{43}$$

$$\sum_{i=2}^{n} \left(\frac{1}{2} \lambda_i^2 \right)^{1-\varpi_2} \leq \sum_{i=2}^{n} \frac{1}{2} \lambda_i^2 + \varpi_2 (1 - \varpi_2)^{\frac{1-\varpi_2}{\varpi_2}}, \tag{44}$$

$$\sum_{i=1}^{n} \left(\frac{1}{2} \tilde{\theta}_{i,j}^{\mathsf{T}} \tilde{\theta}_{i,j} \right)^{1-\varpi_{3,j}} \leq \sum_{i=1}^{n} \frac{1}{2} \tilde{\theta}_{i,j}^{\mathsf{T}} \tilde{\theta}_{i,j} + \varpi_{3,j} (1 - \varpi_{3,j})^{\frac{1-\varpi_{3,j}}{\varpi_{3,j}}}. \tag{45}$$

Moreover, by Lemma 4, it follows that

$$-\sum_{i=1}^{n} \left(\frac{1}{2} z_i^2 \right)^{1-\varpi_1} \leq -\left(\sum_{i=1}^{n} \frac{1}{2} z_i^2 \right)^{1-\varpi_1}, \tag{46}$$

$$-\sum_{i=2}^{n} \left(\frac{1}{2} \lambda_i^2 \right)^{1-\varpi_2} \leq -\left(\sum_{i=2}^{n} \frac{1}{2} \lambda_i^2 \right)^{1-\varpi_2}, \tag{47}$$

$$-\sum_{i=1}^{n} \left(\frac{1}{2} \tilde{\theta}_{i,j}^{\mathsf{T}} \tilde{\theta}_{i,j} \right)^{1-\varpi_{3,j}} \leq -\left(\sum_{i=1}^{n} \frac{1}{2} \tilde{\theta}_{i,j}^{\mathsf{T}} \tilde{\theta}_{i,j} \right)^{1-\varpi_{3,j}}. \tag{48}$$

Combining Equations (43)–(48) yields

$$-\sum_{i=1}^{n}\frac{1}{2}z_i^2 \le -\left(\sum_{i=1}^{n}\frac{1}{2}z_i^2\right)^{1-\varpi_1} + \varpi_1(1-\varpi_1)^{\frac{1-\varpi_1}{\varpi_1}}, \tag{49}$$

$$-\sum_{i=2}^{n}\frac{1}{2}\lambda_i^2 \le -\left(\sum_{i=2}^{n}\frac{1}{2}\lambda_i^2\right)^{1-\varpi_2} + \varpi_2(1-\varpi_2)^{\frac{1-\varpi_2}{\varpi_2}}, \tag{50}$$

$$-\sum_{i=1}^{n}\frac{1}{2}\tilde{\theta}_{i,j}^{\mathsf{T}}\tilde{\theta}_{i,j} \le -\left(\sum_{i=1}^{n}\frac{1}{2}\tilde{\theta}_{i,j}^{\mathsf{T}}\tilde{\theta}_{i,j}\right)^{1-\varpi_{3,j}} + \varpi_{3,j}(1-\varpi_{3,j})^{\frac{1-\varpi_{3,j}}{\varpi_{3,j}}}. \tag{51}$$

In view of Equations (49)–(51), it follows from Equation (42) that Equation (25) holds.

Without loss of generality, assume that the $\hbar$-th subsystem is active before the switching instant t_k. Then, it follows that

$$V_j(t_k) - \mu V_\hbar(t_k^-) = \frac{1}{2\kappa}\sum_{i=1}^{n}(\tilde{\theta}_{i,j}^{\mathsf{T}}\tilde{\theta}_{i,j} - \mu\tilde{\theta}_{i,\hbar}^{\mathsf{T}}\tilde{\theta}_{i,\hbar}) + \frac{1}{2}(z^2 - \mu z^2) + \frac{1}{2}(\lambda^2 - \mu\lambda^2). \tag{52}$$

where $z = [z_1,\ldots,z_n]^{\mathsf{T}}$ and $\lambda = [\lambda_2,\ldots,\lambda_n]^{\mathsf{T}}$. Noting that $\tilde{\theta}_{i,j} = \tilde{\theta}_{i,j} - \frac{1}{2}\tilde{\theta}_{i,\hbar} + \frac{1}{2}\tilde{\theta}_{i,\hbar}$ and recalling that $\mu \ge 1$, inequality (Equation (52)) can be equivalently rewritten as Equation (26).

Remark 5: Unlike conventional backstepping approaches, the proposed virtual control law α_i incorporates mode-dependent control gains $l_{i,j}$ and the gain-related parameters $g_{i,m}$. This structure allows the controller parameters to be adjusted according to the active subsystem, offering greater design flexibility than a common-gain configuration. However, the mode-dependent design may introduce discontinuities in the virtual control signals at switching instants. Their boundedness must therefore be examined when establishing the stability of the switched closed-loop system.

Remark 6: The virtual control laws depend on the active subsystem through the adaptive estimates and design parameters, and may therefore exhibit discontinuities at switching instants. Since $M_{i-1}(\cdot) = -\dot{\alpha}_{i-1}$ is defined along intervals with a fixed active mode, it may be undefined at switching instants. Moreover, the boundedness of the virtual control signals alone does not guarantee that $M_{i-1}(\cdot)$ is uniformly bounded. If the corresponding one-sided time derivatives remain uniformly bounded along the admissible trajectories, a finite constant $M_{i-1}^* > 0$ can be chosen such that $|M_{i-1}(\cdot)| \le M_{i-1}^*$ on all switching-free intervals.

Appendix B. Proof of Theorem 1

Proof of (S1): By Lemma 1, together with Equation (25)–(26), it follows that $V(T) \le (V_{\sigma(0)}^{\rho}(0) + \frac{d_2}{\mu-1})\mu^{N_0}e^{\frac{T\ln\mu}{\tau_d}} - \frac{d_2}{\mu-1} - \omega\rho T$. Hence, the Lyapunov function $V(t)$ remains bounded for all $t \in [0,T)$. According to Equation (24), the boundedness of $V(t)$ implies that the signals $z_1,\ldots,z_n$, $\lambda_2,\ldots,\lambda_n$, as well as the parameter estimation errors $\tilde{\theta}_{i,j}$, $i = 1,\ldots,n$, $j = 1,\ldots,m$, are all bounded. Furthermore, in view of Assumption 1, the transformed system states $s_1,\ldots,s_n$ are bounded. Owing to the switching-dependent model transformation (Equation (17)), the constrained switched system is equivalent to the transformed unconstrained system. Consequently, the original system states $\eta_1,\ldots,\eta_n$ are also bounded. Following standard arguments in [36,37], it can be further concluded that the virtual control signals α_i, the actual control input u, and the nonlinear functions $f_{i,\sigma}(\bar{\eta}_i,\eta_{i+1})$ and $f_{n,\sigma}(\bar{\eta}_n,u)$ remain bounded on $[0,T)$. Therefore, all closed-loop signals of system (Equation (1)) are bounded on $[0,T)$.

Proof of (S2) and (S3): Due to the discontinuity of the switching-dependent PPBs at switching instants, it is necessary to verify whether the tracking error $e_y(t)$ satisfies the prescribed constraints. At each switching instant, Equation (17) and the uniform boundedness of $\bar{T}'_{j,\hbar}(\varepsilon_\hbar)$ imply that the transformed error associated with the newly activated subsystem remains finite. Applying the inverse transformation of Equation (15) then yields

$$-\delta_{\min} < \frac{e_y(t_k^+)}{Q_j(t_k)} < \delta_{\max}.$$

Hence, the prescribed performance constraint is preserved across subsystem switching. From Lemma 5, it follows that along the closed-loop trajectories, the Lyapunov function V_j satisfies Equation (25) during switching intervals and Equation (26) at switching instants. By invoking Lemma 1 and under the ADT condition $\tau_d > \frac{\ln \mu}{\omega \rho}$, the finite-time convergence of $V(t)$ is guaranteed. This condition ensures that the tracking error $e_y(t)$ converges to the residual set within a finite time. Since all closed-loop signals are bounded, the prescribed performance constraint on the tracking error is always satisfied. According to the switching-dependent PPBs Equation (14), the coordinate transformation (Equation (18)), and the first-order filter (Equation (19)), the transformed error system converges practically in finite time. In particular, the convergence time to the residual set is explicitly characterized by Equation (7), which completes the proof.

References

[1] Cheng J, Huang J, Lin X. Output feedback stabilization of networked switched nonlinear systems with continuous-time observers and inter-sample output predictors. *ISA Trans.* 2025, 167:638–645.

[2] Xie J, Chen M, Yang D. Switched-observer-based adaptive neural network secure funnel control of switched nonlinear systems under DoS attacks via event-triggered approach. *Neurocomputing* 2026, 697(C):134139.

[3] Li Y, Tong S. Command-filtered-based fuzzy adaptive control design for mimo-switched nonstrict-feedback nonlinear systems. *IEEE Trans. Fuzzy Syst.* 2017, 25(3):668–681.

[4] Niu B, Ahn CK, Li H, Liu M. Adaptive control for stochastic switched nonlower triangular nonlinear systems and its application to a one-link manipulator. *IEEE Trans. Syst. Man Cybern.: Syst.* 2018, 48(10):1701–1714.

[5] Shi Y, Sun X. Bumpless transfer control for switched linear systems and its application to aero-engines. *IEEE Trans. Circuits Syst. I Regul. Pap.* 2021, 68(5):2171–2182.

[6] Wei C, Chen Q, Liu J, Yin Z, Luo J. An overview of prescribed performance control and its application to spacecraft attitude system. *Proc. Inst. Mech. Eng., Part I: J. Syst. Control Eng.* 2021, 235(4):435–447.

[7] Vrabel R. Event-triggered adaptive learning control for switched discrete-time systems via Lyapunov envelopes. *J. Franklin Inst.* 2026, 363(12):108795.

[8] Jang SG, Yoo SJ. Quantization-based distributed design strategy for adaptive consensus tracking of asynchronously switched nonlinear multiagent systems. *Nonlinear Anal. Hybrid Syst.* 2024, 53:101488.

[9] Shu F, Li M, Liu X, Zhai J. A linearization framework of switched nonlinear systems with input delay. *J. Franklin Inst.* 2026, 363(11):108781.

[10] Bechlioulis CP, Rovithakis GA. A low-complexity global approximation-free control scheme with prescribed performance for unknown pure feedback systems. *Automatica* 2014, 50(4):1217–1226.

[11] Li Z, Ma Y, Yue D, Zhao J. Adaptive tracking for uncertain switched nonlinear systems with prescribed performance under slow switching. *IEEE Trans. Syst. Man Cybern.: Syst.* 2022, 52(11):7279–7288.

[12] Fotiadis F, Rovithakis GA. Prescribed performance control for discontinuous output reference tracking. *IEEE Trans. Autom. Control* 2021, 66(9):4409–4416.

[13] Li R, Yang T, Liu Q, Ma N, Yang Y. Switched prescribed-time extended state observer-based tracking control of a class of nonlinear systems with input delay. *J. Franklin Inst.* 2026, 363(9):108672.

[14] Ma H, Zhou Q, Li H, Lu R. Adaptive prescribed performance control of a flexible-joint robotic manipulator with dynamic uncertainties. *IEEE Trans. Cybern.* 2022, 52(12):12905–12915.

[15] Na J. Adaptive prescribed performance control of nonlinear systems with unknown dead zone. *Int. J. Adapt. Control Signal Process.* 2012, 27(5):426–446.

[16] Wu F, Lian J, Wang D, Zhai G. Prescribed performance bumpless transfer control for switched large-scale nonlinear systems. *IEEE Trans. Syst. Man Cybern.: Syst.* 2023, 53(8):5139–5148.

[17] Yong K, Chen M, Shi Y, Wu Q. Flexible performance-based robust control for a class of nonlinear systems with input saturation. *Automatica* 2020, 122:109268.

[18] Liu L, Liu Y, Tong S. Fuzzy-based multierror constraint control for switched nonlinear systems and its applications. *IEEE Trans. Fuzzy Syst.* 2018, 27(8):1519–1531.

[19] Chen Z, Liu G. Finite-time decentralized bounded L1 control for interconnected positive switched systems under DETM. *J. Franklin Inst.* 2026, 363(10):108734.

[20] Sun K, Guo R, Qiu J. Fuzzy adaptive switching control for stochastic systems with finite-time prescribed performance. *IEEE Trans. Cybern.* 2022, 52(9):9922–9930.

[21] Yu X, Yin J, Khoo S. Generalized Lyapunov criteria on finite-time stability of stochastic nonlinear systems. *Automatica* 2019, 107:183–189.

[22] Mapui A, Mukhopadhyay S. Lyapunov-like prescribed-time stability of impulsive systems via event & self-triggered impulsive control. *Nonlinear Anal. Hybrid Syst.* 2025, 57:101598.

[23] Bechlioulis CP, Rovithakis GA. Prescribed performance adaptive control for multi-input multi-output affine in the control nonlinear systems. *IEEE Trans. Autom. Control* 2010, 55(5):1220–1226.

[24] Wang F, Chen B, Lin C, Zhang J, Meng X. Adaptive neural network finite-time output feedback control of quantized nonlinear systems. *IEEE Trans. Cybern.* 2018, 48(6):1839–1848.

[25] Ren B, Zhong Q, Chen J. Robust control for a class of nonaffine nonlinear systems based on the uncertainty and disturbance estimator. *IEEE Trans. Ind. Electron.* 2015, 62(9):5881–5888.

[26] Song Q, Song Y. Generalized PI control design for a class of unknown nonaffine systems with sensor and actuator faults. *Syst. Control Lett.* 2014, 64:86–95.

[27] Orlov Y. Finite time stability and robust control synthesis of uncertain switched systems. *SIAM J. Control Optim.* 2004, 43(4):1253–1271.

[28] Li Z, Yue D, Ma Y, Zhao J. Neural-networks-based prescribed tracking for nonaffine switched nonlinear time-delay systems. *IEEE Trans. Cybern.* 2021, 52(7):6579–6590.

[29] Dimanidis IS, Bechlioulis CP, Rovithakis GA. Output feedback approximation-free prescribed performance tracking control for uncertain MIMO nonlinear systems. *IEEE Trans. Autom. Control* 2020, 65(12):5058–5069.

[30] Liu Y, Liu X, Jing Y. Adaptive neural networks finite-time tracking control for non-strict feedback systems via prescribed performance. *Inf. Sci.* 2018, 468:29–46.

[31] Chen X, Li J, Wu J, Yi J, Li X. Adaptive neural dynamic surface control with fixed-time prescribed performance for uncertain nonstrict-feedback stochastic switched systems. *Nonlinear Anal. Hybrid Syst.* 2023, 48:101334.

[32] Corless RM, Gonnet GH, Hare DE, Jeffrey DJ, Knuth DE. On the Lambert W function. *Adv. Comput. Math.* 1996, 5(1):329–359.

[33] Chen G, Yang Y. Finite-time stability of switched nonlinear time-varying systems via indefinite Lyapunov functions. *Int. J. Robust Nonlinear Control* 2018, 28(5):1901–1912.

[34] Sun Y, Chen B, Lin C, Wang H, Zhou S. Adaptive neural control for a class of stochastic nonlinear systems by backstepping approach. *Inf. Sci.* 2016, 369:748–764.

[35] Cai M, Xiang Z. Adaptive neural finite-time control for a class of switched nonlinear systems. *Neurocomputing* 2015, 155:177–185.

[36] Zhao Q, Chen X, Li J, Wu J. Finite-time adaptive fuzzy DSC for uncertain switched systems. *Int. J. Fuzzy Syst.* 2020, 22:2258–2270.

[37] Swaroop D, Hedrick JK, Yip PP, Gerdes JC. Dynamic surface control for a class of nonlinear systems. *IEEE Trans. Autom. Control* 2000, 45(10):1893–1899.